Morphodynamics of a growing microbial colony driven by cell death

Pushpita Ghosh[1,*] and Herbert Levine[2,3]
[1]*Centre for Interdisciplinary Sciences, Tata Institute of Fundamental Research, Hyderabad 500107, India*
[2]*Center for Theoretical Biological Physics, Rice University, Texas 77005, USA*
[3]*Department of Bioengineering, Rice University, Texas 77005, USA*
(Received 6 February 2017; revised manuscript received 20 July 2017; published 8 November 2017)

Bacterial cells can often self-organize into multicellular structures with complex spatiotemporal morphology. In this work, we study the spatiotemporal dynamics of a growing microbial colony in the presence of cell death. We present an individual-based model of nonmotile bacterial cells which grow and proliferate by consuming diffusing nutrients on a semisolid two-dimensional surface. The colony spreads by growth forces and sliding motility of cells and undergoes cell death followed by subsequent disintegration of the dead cells in the medium. We model cell death by considering two possible situations: In one of the cases, cell death occurs in response to the limitation of local nutrients, while the other case corresponds to an active death process, known as apoptotic or programmed cell death. We demonstrate how the colony morphology is influenced by the presence of cell death. Our results show that cell death facilitates transitions from roughly circular to highly branched structures at the periphery of an expanding colony. Interestingly, our results also reveal that for the colonies which are growing in higher initial nutrient concentrations, cell death occurs much earlier compared to the colonies which are growing in lower initial nutrient concentrations. This work provides new insights into the branched patterning of growing bacterial colonies as a consequence of complex interplay among the biochemical and mechanical effects.

DOI: 10.1103/PhysRevE.96.052404

I. INTRODUCTION

Microbial colonies are the most widely studied multicellular organizations in the realm of living matter. From an individual cell or a small cellular aggregate, a complex multicellular spatial structure can develop. In some cases this structure is commonly known as biofilm, in which bacterial cells adhere to each other while being embedded in a self-secreted extracellular matrix [1–4]. An expanding microbial colony is influenced by a number of processes, including cellular growth-division, surface attachment-detachment, motility, secretion of extracellular polymeric substances, and mechanical, chemical, and hydrodynamic interactions [5–19]. Moreover, microbial communities very often encounter unfavorable conditions around their natural environment, such as nutrient limitation, presence of competitors, and harmful chemicals during antibiotic treatment [20–23].

One of the characteristic processes associated with a developing multicellular organization is cell death [2,4,20,22,24–27], which is one of the least understood among the aforementioned processes. Different forms of cell death in bacteria have been reported in previous studies [20–22,27,28]. It has been shown that *Bacillus subtilis* delays sporulation by killing and thereby supplying food for their nonsporulating siblings to prevent unnecessary spore formation [20,22,29–31]. Recent experimental studies have emphasized the role of heterogeneous cell death on spatial morphology in a *B. subtilis* biofilm [4,14].

More generally, in a bacterial population, responding to adverse conditions, cells can regulate the death program for the benefit of the overall colony. Programmed cell death (PCD) is one such process, defined as an active mechanism that results in cell suicide [21,22,32–34]. It has been reported that on amino acid starvation, *Escherichia coli* undergoes programmed altruistic death, during which the dying cells provide nutrients for the survival of other cells [35,36]. In Refs. [37,38], the presence of significant amounts of extracellular DNA within *Pseudomonas aeruginosa* biofilm provides strong evidence of PCD and lysis of the dead cells during biofilm formation. Overall, the understanding of the underlying causes, mechanisms, and subsequent role of various cell-death processes remains largely unexplored.

Depending on the particular bacterial species and environmental conditions, a wide variety of morphological patterns can emerge. For instance, *B. subtilis* exhibits different types of patterns, ranging from disklike colonies to dense or sparse branched morphology, including diffusion-limited aggregation-like patterns, compact Eden-like structures, and concentric ringlike morphologies [39,40]. Attempts have been made towards understanding the occurrence of different morphological instabilities and the concomitant pattern formation, both experimentally and theoretically. Earlier studies have revealed that the discrete nature of bacteria and inherent fluctuations can be responsible for the diffusive instabilities leading to the roughening of expanding fronts in growing colonies [41,42]. A cutoff based reaction-scheme was employed in those studies to explain such roughening. Moreover, Golding and coworkers has pointed out that the role of a death term in cut-off-based reaction-diffusion model is to stabilize the branching instability [43]. However, a sophisticated model which automatically takes care of the discrete particle nature and the fluctuations and couples them to microbial growth dynamics is still elusive.

In this regard, the key questions that we want to explore in the present study are as follows:

(i) How and to what extent might nutrient depletion induced cell death affect the growth and morphology of a developing colony?

*pghosh@tifrh.res.in

(ii) What is the role of apoptotic/programmed cell death and to what extent can it regulate the growth dynamics and morphology?

(iii) To what extent can the altruistic aspects of programmed cell death affect the growth dynamics?

The objective of the present study is to model cell death in an expanding bacterial colony to gain an understanding of its influence on growth and morphological dynamics. To address these issues, we first use a cutoff based reaction-diffusion model including cell death and lysis as a prelude. We observe branching instabilities at the colony front. In agreement with the previous works, the cut-of-based reaction term apparently includes at least qualitatively the effect of discreteness and fluctuations in the growing colony [41,42]. However, the main focus of the present work is to construct an individual-based model which automatically takes care of discrete nature of bacterial cells and the resultant inherent fluctuations in the colony. We implement two possible rules for cell death: (1) nutrient-limited cell death: a cell dies if the local nutrient level goes below a certain value; and (2) apoptotic or programmed cell death (PCD): random active cell death, which means cells commit suicide in a random manner with a certain rate. Our study suggests that not only fluctuations are important but also cell death is crucial to develop branching patterns in the colony front. We show that colony morphology depends on the rate and pattern of cell death. In particular, while nutrient limitation alone gives rise to a colony with a rough interface of live peripheral cells moving outwardly, adding death gives rise to an accumulation of dead and disintegrated cells in the interior of the growing colony which now can develop highly branched structures at the periphery. Moreover, we show that initial nutrient concentration plays an interesting role for the local nutrient competition and the initiation of cell death. Our result predicts the emergence of branched morphology in a developing microbial colony mediated by cell death which therefore appears to be a significant factor in the evolution of spatiotemporal order in bacterial colonies.

II. CUT-OFF-BASED REACTION-DIFFUSION MODEL

We consider a mean-field type reaction-diffusion system governing nonmotile bacteria grown on a semisolid agar surface in presence of a diffusing nutrient. We begin with the Kessler-Levine equations [41] as follows:

$$\frac{\partial u}{\partial t} = uv\Theta(u-\epsilon) + D\nabla^2 u, \tag{1}$$

$$\frac{\partial v}{\partial t} = -uv\Theta(u-\epsilon) + \nabla^2 v, \tag{2}$$

where ϵ is the threshold density for growth and Θ is the Heaviside step function [1 if $(u > \epsilon)$ and 0 otherwise]. The concentration of bacteria and nutrient or food are represented by u and v, respectively. The food consumption term is of the form $f(u,v) = uv$, which is a widely used low-nutrient approximation and the parameter $D = 0.01$ represents the ratio of diffusivity of bacteria and nutrient. The cutoff in the reaction term at small bacteria density is used to represent the discreteness of bacteria and fluctuations present in a growing colony which are responsible for the existence of a diffusive instability [41,42]. We carry out numerical simulations of the reaction-diffusion model [Eqs. (1) and (2)] with the zero-flux boundary condition by a Euler method for time marching with a time step of 0.005, and standard finite-difference scheme in a square domain of length $L = 250$ with a grid size of 0.25, for resolving the diffusion. As an initial condition, we consider a small circular inoculation of bacteria with some randomness in its density at the center of the square box and the initial concentration of the nutrient field is kept equal throughout the box. As can be seen from Fig. 1 under a no-death condition, there arises a diffusive instability but deep branching does not occur since emergent dips are quickly healed. It has been suggested that one of the ways to obtain and stabilize the branch formation is to introduce a death term [43].

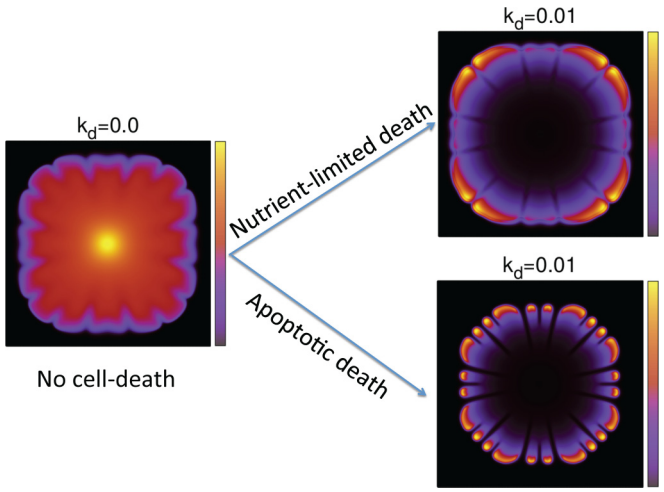

FIG. 1. Snapshot of colonies (alive+dead) in absence and in presence of cell death for a cutoff $\epsilon = 0.2$. For both the cases of nutrient-limited death and apoptotic death, value of the rate of cell death is $k_d = 0.01$ and rate of lysis of the dead cells is $k_{\rm lys} = 0.002$. Shown here is the snapshot of a simulated colony in case of nutrient-limited cell death, which occurs when local nutrient concentration crosses a threshold value of $C_{\rm thresh} = 0.001$. The color bar shows the variation of concentrations from low (blue) to high (yellow); black corresponds to a zero value.

To include the effect of cell death and subsequent lysis, we here consider a modified model as follows:

$$\frac{\partial u}{\partial t} = uv\Theta(u-\epsilon) - k_d u + D\nabla^2 u, \tag{3}$$

$$\frac{\partial v}{\partial t} = -uv\Theta(u-\epsilon) + \nabla^2 v, \tag{4}$$

$$\frac{\partial w}{\partial t} = k_d u - k_{\rm lys} w, \tag{5}$$

where k_d is the rate of cell death which leads to the accumulation of a dead and inactive population of bacteria represented by $w(x,y,t)$. These eventually disintegrate with time at a constant rate $k_{\rm lys}$. We now carry out numerical simulations of the reaction-diffusion model [Eqs. (3) to (5)] following the aforementioned method for different values of the cell death rate k_d, at a fixed rate of cell-lysis $k_{\rm lys} = 0.002$. We observe enhanced branching patterns at the colony periphery on increasing k_d, as can be seen from Fig. 1. Specifically, under

the condition of nutrient-dependent cell death, we assume a threshold concentration of nutrients, $C_{\text{thresh}} = 0.001$, below which the cell starts to die. Therefore, we multiply the death term $k_d u$ of Eqs. (3) and (5) by a function H such that ($H = 1$ for $v < C_{\text{thresh}}$ or $H = 0$ otherwise). For apoptotic death, cells die randomly from any part of the growing colony.

Apparently, cell death seems to be a significant parameter in branch formation. However, it appears that in the absence of a cut-off term, cell death cannot by itself lead to such branching instabilities at colony fronts (result not shown). This suggests that discreteness and inherent fluctuations play crucial roles in causing cause front instabilities. Cell death accompanies fluctuation-driven instability to create enhanced branching. The underlying reason here lies in the fact that bacteria left behind the propagating front become dead and inactive. They are unable to move to close the emerging dips, thus allowing deep branches to form.

Although the above cut-of-based continuum model has been able to show branch formation, a more sophisticated methodology and a better model is a necessity to quantitatively account for the discrete particle nature and the inherent fluctuations in an expanding colony. In this regard, we use an individual-based or agent-based model of expanding a microbial colony which by its very nature takes care of the discreteness of cells and inherent fluctuations present in a colony. In the following section, we will describe our individual-based model including the presence of cell death.

III. THE INDIVIDUAL-BASED MODEL AND METHOD

Next, we consider colony dynamics by means of individual-based modeling [11,15]. In our model, an individual bacterial cell is considered as a nonmotile growing spherocylinder having constant diameter ($d_0 = 1\mu$m) and variable length l. We consider a two-dimensional (2D) semisolid surface ($300\ \mu\text{m} \times 300\ \mu\text{m}$) for colony growth and therefore each cell is represented by a spatial coordinate $r = (x, y)$ and unit vectors (u_x, u_y) representing the orientation of the symmetry axis of the cell. The growth of a cell depends on the availability of local nutrients which are diffusing in the medium. The two-dimensional surface is discretized into equally sized square units. Each square patch is characterized by a nutrient concentration $c(x, y)$. As the simulation of local nutrient competition between individual cells is one of the primary goals, the patch dimension is presumed to be in the same order of magnitude as the microbial cell size, more specifically $2\ \mu$m. The colony expands due to the utilization of local nutrient governed by a diffusion equation linked to a sink term which reflects the nutrient consumption by the cells,

$$\frac{\partial c}{\partial t} = D\left(\frac{\partial^2 c}{\partial x^2} + \frac{\partial^2 c}{\partial y^2}\right) - k\sum A_i f(c(x_i, y_i)), \qquad (6)$$

where $A_i = \pi r_0^2 + 2r_0 l_i$ is the area of cell i, $r_0 = d_0/2$ is the radius of the end cap, l is the length of the cell, and x_i, y_i is its spatial coordinates. Initially, the nutrient concentration has been taken to be $c = C_0$ everywhere and c is kept constant at the edges of the simulation box, which is taken large enough to ensure that there is no direct effect of the boundaries. The nutrient is utilized by the bacterial cells at a rate $kf(c)$ per unit biomass density where $f(c)$ is a monotonically increasing dimensionless function. In our simulations, we assume $f(c) = c/(1 + c)$, a Monod function with half-saturation constant equal to 1 (in arbitrary units).

In our model, a cell i grows by elongation in accordance with the relation $dl_i/dt = \phi.(A_i/\bar{A}).f(c(x_i, y_i))$, where ϕ is the constant growth parameter and $\bar{A} = \pi r_0^2 + \frac{3}{2} r_0 l_{\max}$ is the average area [11,15] in a two-dimensional representation. This is equivalent to assuming that the cells grow at a rate proportional to the biomass or volume of a cell [44] and taking the volume to be simply a fixed height times the two-dimensional area. An alternative could be to compute the real 3D volume of an assumed spherocylinder which yields a slightly different formula; we expect that this change would make only very minor changes in our results. One consequence of including the cell area A_i in the above relation is that it ensures that the colony grows at the same rate for cells with different average aspect ratios.

Once a cell reaches a critical length $l_{\max}$, it splits at a rate k_{div} into two independent daughter cells with orientations roughly the same as the mother cell but with small randomness. This randomness in the orientation incorporates the effect of various irregularities in the system, e.g., roughness of the agar surface, slight bending of the cells, etc. This stochasticity allows for quasicircular colony growth instead of cells growing as long filaments. We assume cells interact directly by mechanical interactions in accordance with the Hertzian theory of elastic contact [8,10] by repelling neighboring cells in case of spatial overlap. The force between two spherocylinders is approximated by the force between two spheres placed along the major axis of the rods at such positions that their distance is minimal [15]. If the shortest distance between the two spherocylinders is r and $h = d_0 - r$ is the overlap, then the force is assumed to be $F = E d_0^{1/2} h^{3/2}$, where E parametrizes the strength of the repulsive interaction proportional to the elastic modulus of the cell. $E \longrightarrow \infty$ implies perfectly hard cells but in fact our simulation uses a finite value of E (see Table I), allowing for some deformation. In addition to direct intercellular interaction there is competition for nutrient, which can be considered as indirect interaction between microbial cells mediated by the environment. In such a dense system, inertia can be neglected and we consider the overdamped

TABLE I. Parameters and constants used in the simulations.

Parameter	Symbol	Simulations
Maximum length	$l_{\max}$	$4.0\ \mu$m
Diameter of cell	d_0	$1.0\ \mu$m
Linear growth rate	ϕ	$1.5\ \mu\text{m h}^{-1}$
Cell-division rate	k_{div}	$0.2\ \text{h}^{-1}$
Cell death rate	k_d	0.00075–$0.005\ \text{h}^{-1}$
Lysis rate of dead cells	k_{lys}	$1.0\ \text{h}^{-1}$
Elastic modulus of alive cells	E	3×10^5 Pa
Elastic modulus of dead cells	E_d	10^4 Pa
Friction coefficient	ζ	200 Pa h
Initial nutrient concentration	C_0	$0.5\ \text{fg}\ \mu\text{m}^{-3}$
Nutrient consumption rate	k_c	$6.0\ \text{h}^{-1}$
Diffusion rate of nutrient	D	$400\ \mu\text{m}^2\ \text{h}^{-1}$

dynamics for the cellular motion. The equations of motion are given by

$$\dot{\mathbf{r}} = \frac{1}{\zeta l}\mathbf{F}, \tag{7}$$

$$\omega = \frac{12}{\zeta l^3}\tau, \tag{8}$$

where ζ is the friction per unit length of cell and r and ω are position and the cells angular velocity, respectively. The corresponding linear forces and torques are represented by F and τ.

We implement cell death in a growing colony following two possible scenarios:

Method 1: nutrient-depletion mediated cell death. In this case we assume that the nutrient level going below a certain threshold triggers cell death. This assumes that when bacteria are starving they start dying in response, without making any active apoptotic decision.

Method 2: apoptotic or programmed cell death. In this approach we assume that some of the bacterial cells decide to undergo random death, quite similar to what happens in eukaryotic multicellular systems.

To explore the role of dead cells in governing colony dynamics, it is necessary to investigate both the mechanical properties and the effect of lysis of the dead cells. We typically consider the dead cells to have a low repulsive elastic coefficient as compared to that of alive cells. Furthermore, we assume that dead cell undergoes lysis following a shrinking of its size at a certain rate; eventually it will disintegrate completely and subsequently get removed from the colony. To understand the combined effect of weaker forces and lysis, we carry out several controlled variations on our simulations: (i) keeping the mechanical interactions the same as for alive cells as long as the dead cells have not yet completely disintegrated and been removed from the system, (ii) lowering the mechanical repulsive forces of dead cells but not allowing them to disintegrate, (iii) keeping the repulsive mechanical forces of dead cells the same as for alive cells but including the fact that dead cells undergo rapid lysis. These are discussed in the following section.

IV. RESULTS AND DISCUSSION

The main focus of the current study is to understand the role of cell death determining the dynamics and morphology of a growing bacterial colony. We begin our study by simulating a few number ($N = 5$) of bacterial cells attached to a two-dimensional surface and explore how the colony develops. Microbial cells uptake local nutrient available in the medium in order to grow, divide, and spread by mechanically driven sliding motility. First, we ignore cell death. The colony expands from the center of the two-dimensional simulation box, leading to nutrient depletion in the interior region due to the increase in the local cell density. As a result, the growth of the cells in the interior region becomes slower. We see that a roughly circular colony develops as shown in Supplemental Movie 1 in Supplemental Material [45] and also demonstrated in the snapshots in Fig. 2 under no death condition.

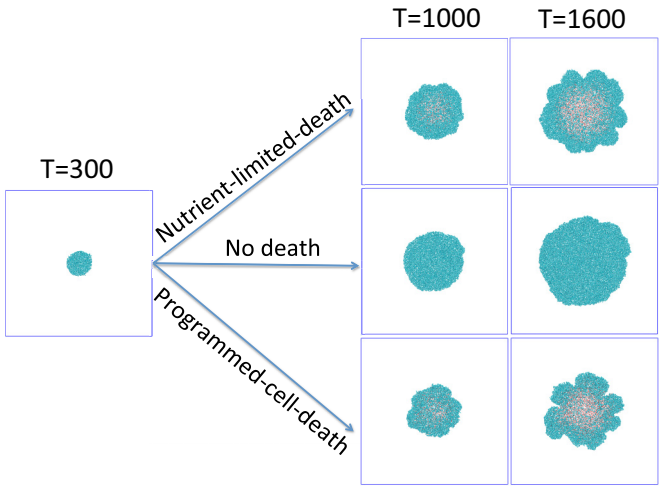

FIG. 2. Spatiotemporal morphology of the growing colonies with respect to time in presence and absence of cell death. For both the cases of nutrient-limited death and programmed cell death, the rate of cell death is $k_d = 0.001$. Shown here are the snapshots of a simulated colony which occurs for a threshold concentration of the local nutrient level $C_{\text{thresh}} = 0.001$ in the case of nutrient-limited cell death. Programmed cell death occurs randomly without any concentration threshold of the nutrient concentration. Here alive cells are represented by spherocylinders (cyan) and dead and disintegrated cells are depicted in the form of tiny red dots. All the other parameters are chosen to be same as given in the Table I.

Next, we implement cell death considering the following two processes: nutrient-depletion-driven cell death and apoptotic or programmed cell death. For the process of *nutrient-depletion-driven cell death*, we implement the possibility of nutrient-limited death after initial colony development up to time $T = 300$ h. When the local nutrient level falls below a certain threshold value, which we choose in the simulations as $C_{\text{thresh}} = 0.001$ fg/μm^3, the starving cells cannot cope with the nutrient-deficient condition and start to die. As already mentioned, once cell death occurs, the dead cells disintegrate at a fixed rate until they disappear from the colony. Supplemental Movie 2 in Supplemental Material [45] demonstrates the colony development in the presence of nutrient-dependent-cell death. The corresponding snapshots of simulated growing colony with respect to time are shown in Fig. 2 under the nutrient-limited death condition. We observe a roughly circular band of live cells that grows outward, keeping the dead and disintegrated cells in the interior region since the nutrient comes from the edges of the simulation box. Moreover, we find that the spatiotemporal morphology at the colony edge undergoes a clear transition from roughly circular to a branched structure as time progresses.

On the other hand, similarly to what occurs in eukaryotic multicellular systems, *apoptotic or programmed cell death* might occur in a multicellular bacterial populations. The underlying mechanism of apoptotic or PCD is different depending on the type of stress involved in the particular microbial colony. Why and how bacteria switch on suicide program is poorly known. Our objective here is to predict the significance of programmed cell death in a growing colony without specifying in detail any particular mechanism. To understand and compare

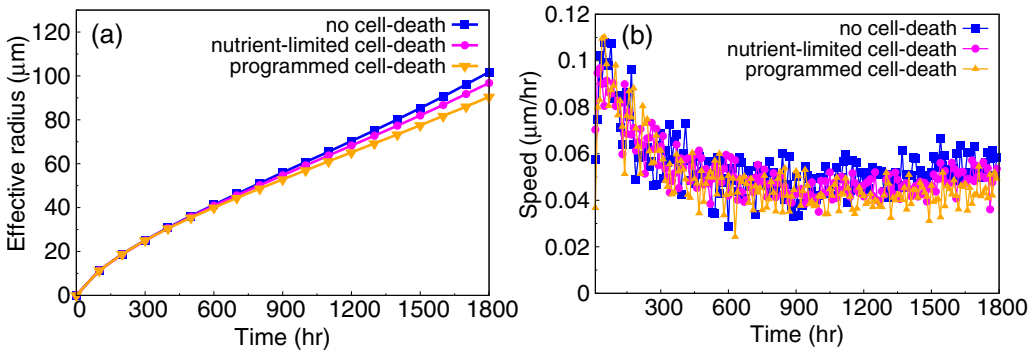

FIG. 3. (a) Plot of effective radius of the growing colonies with respect to time. (b) Plot of the speed of the colony with respect to time. The blue curve (with filled squares) corresponds to no-death situation, whereas the magenta (with filled circles) and orange (with filled triangles) curves correspond to nutrient-limited and programmed cell death, respectively. Rate of nutrient-limited and programmed cell death is $k_d = 0.001$ and all the other parameters are same as given in the Table I.

the role of apoptotic or PCD in a growing colony, we impose random cell death with a fixed rate in our simulations after the colony grows to time $T = 300$ h. Supplemental Movie 3 in Supplemental Material [45] demonstrates the simulation result of a growing colony in presence of apoptotic death which is also elucidated in Fig. 2 under the condition of programmed cell death. PCD occurs randomly from any part of the colony irrespective of the local nutrient availability. As time goes on, in the colony center (mostly) the cells stop their growth and division, dead cells accumulate, and the expanding front shows a transition from roughly circular to a highly branched morphology at the colony edge.

As we can observe the development of branched structures at the colony edges in presence of cell death, it is useful to investigate in detail how the colony morphology depends on the presence of cell death. What are the characteristic properties that can imply the certain role of cell death in a growing colony governing its morphological dynamics? To answer these questions, we now compute the time profile of effective radius of a growing colony and speed of the colony front in the presence and absence of cell death. The effective radius as time progresses as shown in Fig. 3(a), which reveals that colony spreading is only slightly reduced in the presence of cell death. This is directly shown in results for the speed of the colony front in Fig. 3(b).

It is now necessary to quantify how cell death governs the morphology of the growing colony. As we have seen in Fig. 2, the colony edge develops more branches as the number of dead cells increases with time. To quantify the effect of cell death in shaping colony morphology, we determine a roughness parameter(σ_f) characterized by the standard deviation of the distance of the peripheral cells from the center of the box. We plot the time profile of σ_f, which is an ensemble average of multiple simulation data as illustrated in Fig. 4(a) for the three different cases: no death, nutrient-dependent death, and programmed cell death. The increase in the value of roughness parameter with respect to time clearly indicates that, in the presence of cell death, bacteria develop highly branched structures at the periphery of the colony. At the same time, we observe that σ_f is higher in the case of programmed cell death as compared to nutrient-dependent death.

We furthermore investigate how the roughness parameter depends on the rate of cell death. In Fig. 4(b), we plot the ensemble average value of the roughness parameter for different values of rate of cell death k_d after the colony grows for a sufficiently long time. We see that with the increased rate of cell death, σ_f monotonically increases up to a certain limit and then saturates to a plateau for higher values of cell death rate. These observations clearly suggest that cell death can influence the colony morphology by facilitating transitions from circular to branched structures in multicellular growing systems. For nutrient-limited death, at higher values of cell death rate k_d, it appears that only the microbial cells at the colony periphery will grow as a band and the interior will consist entirely of the dead and disintegrated cells. On the other hand, for high apoptotic cell death rate, the colony becomes very sparse with the presence of dead cells and their removal by disintegration. For very high values of apoptotic cell death, the whole colony can collapse.

We now focus on the possible role of altruism in programmed cell death. We now assume that dying cells can provide nutrients to the other cells as a way of helping them to overcome nutrient limitation. First, we calculate for the given parameter set how much nutrient is consumed by an individual bacterial cell as it grows to the maximal threshold length; this equals 12–14 fg for our given parameter set. We presume that nutrient deposition by a dead cell must be less than what it required for growth. Based on these facts, we have chosen an approximate value of nutrient production by the dead cells. We consider two different approaches in order to understand the prospective behavior of the colony in presence of altruistic death. In the first approach we suppose that dead cells during lysis deposit nutrient in the medium continuously until they completely disintegrate with a rate $k_{\rm np} = 3.0$ corresponding to the total deposition of 8 fg of nutrient per dead cell in the medium. In the second approach, dead cells disintegrate or undergo lysis with a rate $k_{\rm lys} = 1.0$ and, after complete disintegration, an amount of metabolite or nutrient is deposited abruptly into the growth medium. Nutrient deposition by dead cells in the local regions allows the remaining neighboring alive cells to utilize the deposited nutrient to grow and survive the nutrient depletion for longer time. Apparently, there is

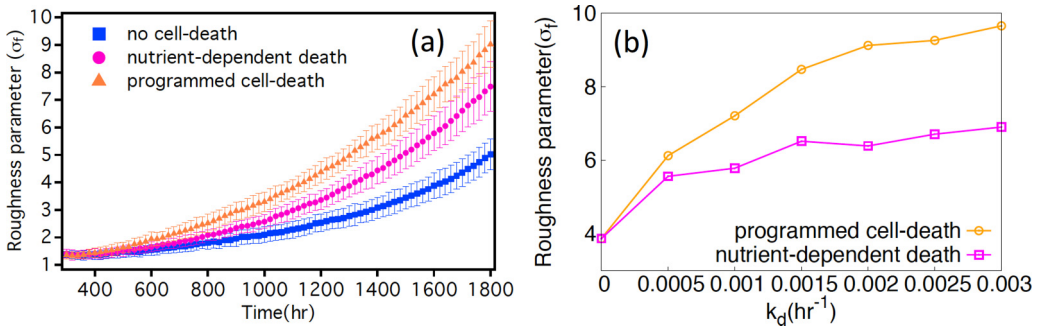

FIG. 4. Roughness parameter σ_f, which is determined by calculating the variance in radius of the peripheral bacterial cells of the expanding colonies with respect to time for (a) no death (filled blue squares), nutrient-dependent death (filled magenta circles), and programmed cell death (filled orange triangles). The cell death rate is taken as $k_d = 0.001$. (b) Plot of averaged values of roughness parameter σ_f from multiple realizations of simulation trajectories as a function of death rate k_d for programmed cell death (orange curve with empty triangles) and nutrient-dependent cell death (magenta curve with empty squares). All the other parameters are same as given in the Table I.

no significant difference noticeable in the morphology of the spatiotemporal dynamics due to the inclusion of altruism (data not shown). However, if we calculate covered area of the live cells with respect to time for all the three cases: (a) cell death without nutrient production, (b) cell death with continuous nutrient production by dead cells until it completely disintegrate, and (c) cell death with delayed nutrient production by dead cells after it completely disintegrate, a significant change can be observed in the number of live bacterial cells, as shown in Fig. 5. We found that effective radius which is determined by taking the square root of the covered area of live bacterial cells is not surprisingly higher in cases of altruistic cell death compared to nonaltruistic death, as the released nutrient helps neighboring cells to survive for a longer time.

To better understand the role of mechanical and structural effects of dead cells in regulating colony morphodynamics, we carry out several additional simulations with varied rules. In one of the cases, we allow a dead cell to interact with the same repulsive force as that of live cells as long as it is present in the system. Once it disintegrates there is no longer any repulsive mechanical force. In a second case, the dead cells in the growing colony remain unchanged in their size and shape but have lower elastic repulsive forces ($E_d = 10^4$) of interaction with the neighboring cells. The results of the change of roughness parameter σ_f with respect to time for these simulations are compared with the cases of no cell death in Fig. 6. We observe that having weak repulsive forces of dead cells ($E_d = 10^4$) without their removal gives rise to lower roughness in the colony fronts than removal of dead cells by disintegration. However, if they are given similar repulsive properties as of the live cells, then the dead cells would have a greater impact in creating nonuniformity and sparseness and hence greater roughness in the colony fronts. This appears to be a result of the abrupt loss of strong repulsive forces provided by the dead cells as they vanish from the system. All these

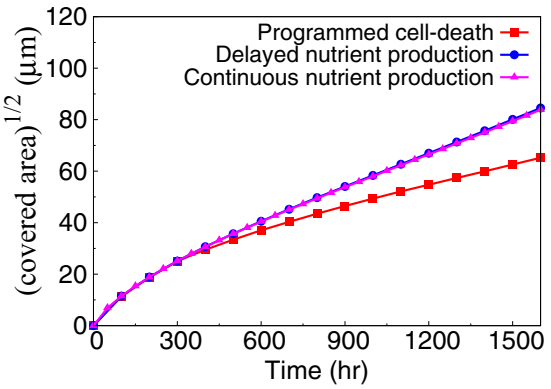

FIG. 5. Plot of square root of covered area of the live cells of the expanding colony with respect to time. The red curve with filled squares corresponds to the case of programmed cell death, whereas the blue curve with filled circles and the magenta curve with filled triangles (which are basically indistinguishable) correspond to the cases of delayed and continuous production of nutrient by the dead cells during programmed death, respectively. For all three cases, the death rate is taken as $k_d = 0.001$. All the other parameters are the same as given in the Table I.

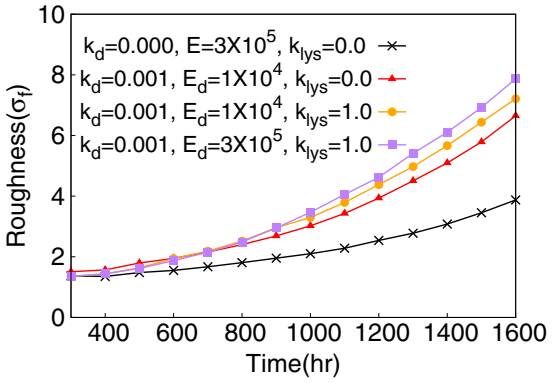

FIG. 6. Roughness parameter σ_f of the expanding colonies with respect to the time. The black curve with crosses corresponds to the case of no death ($k_d = 0.0$) in the colony; the red curve with triangles for programmed cell death ($k_d = 0.001$) with low repulsive coefficients of dead cells ($E_d = 10^4$) without cell lysis ($k_{lys} = 0.0$) and removal; the orange curve with circles corresponds to the case of programmed cell death ($k_d = 0.001$) with low elastic repulsive coefficient of dead cells ($E_d = 10^4$) and their removal from the system ($k_{lys} = 1.0$); and the purple diamond curve shows the case where dead cells have same repulsive coefficient as alive cells ($E_d = E = 3 \times 10^5$) but undergoes lysis ($k_{lys} = 1.0$) and removal from the growing colony. The rate of cell death is $k_d = 0.001$ and all the other parameters are kept same as given in the Table I.

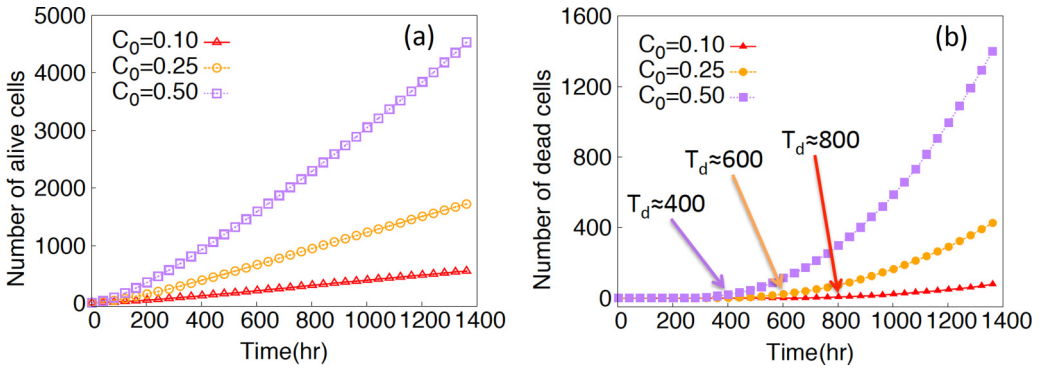

FIG. 7. Effect of initial nutrient concentration (C_0) on initiation of cell death in case of nutrient-dependent death. (a) Plot of total number of alive cells with respect to time for different C_0s. (b) Plot of total number of dead cells with respect to time for different C_0s. The onset of cell death is represented by T_d. All the other parameters are kept as given in Table I in the corresponding simulations.

observations suggests that the loss of repulsive mechanical forces as a result of disintegration and removal of the dead cells from the growing colony is the key factor which causes a transition from circular to branched structures.

To further investigate how the nutrient depletion pattern and hence associated cell death is influenced by the initial nutrient concentration C_0, we carried out simulations varying initial nutrient concentration C_0. We find that with higher initial nutrient concentrations, colony size increases as predicted by the total number of alive cells demonstrated in Fig. 7(a). However, interestingly, our simulations reveal that the cells start to die at a later time while growing in lower initial nutrient concentration C_0, for a given threshold concentration C_{thresh} below which cells start to die. In Fig. 7(b), we plot the temporal evolution of the number of dead cells for three initial nutrient concentrations, which shows that the onset of cell death is triggered at much later time for lower C_0s. It turns out from the observation that cell death depends not only on the local nutrient concentration but also on the local concentration of cells competing for the available nutrient consumption for their growth. In the case of lower C_0, the cell growth is slow, which also results in a lower local cell density of bacterial cells compared to that in higher C_0 at a given time. Hence the extent of competition among cells for nutrient consumption is lower at a lower C_0, resulting in a late onset of cell death.

V. CONCLUDING REMARKS

Over the past few decades, there has been a great deal of interest in understanding multicellular organization in bacteria by studying the individual interactions among cells by using agent-based models. The advantage of these models over mean-field-level descriptions lies in the fact that they automatically take care of the discrete nature of microbial cells and fluctuations at the interfaces. cell death, especially PCD, being one of the important elements of multicellular developmental process, presents both a challenge for basic biological understanding and a potential opportunity for developing effective antibiotic treatment strategies. Although specific mechanisms for cell death in some of these cases have been well characterized [21,27,35], the consequences of such a process for a developing multicellular community, such as a biofilm, has been difficult to explore experimentally.

In this article, using an individual-based model, we investigate the role of cell death in an expanding bacterial colony on a semisolid agar surface. How the interplay of cell death and mechanical interactions can effectively govern the morphological features of a growing colony is the key result of the present work. We show how either nutrient-limited death and programmed cell death can significantly influence the growth morphology which is reflected in the spatial behavior by enhanced branch formation at the colony periphery. How the initial nutrient concentration might affect the dynamics is also demonstrated; the results indicate that not only local nutrient concentration but also the local concentration of bacterial cells determines the initiation of cell death (under the condition of nutrient-dependent cell death).

It has been established in previous studies [11,15,46] that a transition from a circular to a branched colony can be driven solely by the uptake of nutrient by bacterial cells and their growth by mechanical pushing; this seems to occur for very slowly moving fronts. However, in our present work, we find that cell death in a mechanically driven growing colony will only slightly modify the effective speed of an expanding colony but it could lead to a significant change in the colony morphology. The underlying reasons appear to be the combined effect of discreteness of cells and inherent fluctuations, a weak repulsive elastic interaction between dead and neighboring cells, and eventual removal of the dead cells from the system through disintegration which creates void spaces in the colony structure.

Our present model is of course in two dimensions and therefore only sheds direct light on the morphological behavior of a monolayer of bacteria. However, in many cases, bacteria can develop three-dimensional multicellular structures [4,10,47]. Extending our work to three dimensions is nontrivial as many new features such as the cell-surface interaction resulting from symmetric or asymmetric adhesion of anisotropic bacteria with the substrate might also influence the structure of a colony [48]. Future studies will indeed aim for such an extension and will explore the role of cell death along with these complex cell-surface interactions. Nevertheless, our results suggest that also 3D multicellular systems which have highly branched morphology might be strongly influenced by high cell death during their growth and development.

ACKNOWLEDGMENTS

We thank J. Mondal and P. Perlekar for careful reading of the manuscript and helpful comments. This work is partially supported by DST-INSPIRE Faculty Award (DST/INSPIRE/04/2015/002495). This research was also supported by the NSF (Award No. MCB-1241332) and the NSF-funded Center for Theoretical Biological Physics (Award No. PHY-1427654).

[1] G. A. O'Toole and R. Kolter, Mol. Microbiol. **30**, 295 (1998).
[2] K. W. Bayles, Nat. Rev. Micro. **5**, 721 (2007).
[3] J. W. Costerton, Z. Lewandowski, D. E. Caldwell, D. R. Korber, and H. M. Lappin-Scott, Annu. Rev. Microbiol. **49**, 711 (1995).
[4] M. Asally, M. Kittisopikul, P. Rué, Y. Du, Z. Hu, T. Çağatay, A. B. Robinson, H. Lu, J. Garcia-Ojalvo, and G. M. Süel, Proc. Natl. Acad. Sci. USA **109**, 18891 (2012).
[5] A. Be'er, H. P. Zhang, E.-L. Florin, S. M. Payne, E. Ben-Jacob, and H. L. Swinney, Proc. Natl. Acad. Sci. USA **106**, 428 (2009).
[6] E. Ben-Jacob, I. Cohen, and H. Levine, Adv. Phys. **49**, 395 (2000).
[7] H. Cho, H. Jansson, K. Campbell, P. Melke, J. W. Williams, B. Jedynak, A. M. Stevens, A. Groisman, and A. Levchenko, PLoS Biol. **5**, e302 (2007).
[8] D. Volfson, S. Cookson, J. Hasty, and L. S. Tsimring, Proc. Natl. Acad. Sci. USA **105**, 15346 (2008).
[9] H. P. Zhang, A. Beer, E.-L. Florin, and H. L. Swinney, Proc. Natl. Acad. Sci. USA **107**, 13626 (2010).
[10] D. Boyer, W. Mather, O. Mondragón-Palomino, S. Orozco-Fuentes, T. Danino, J. Hasty, and L. S. Tsimring, Phys. Biol. **8**, 026008 (2011).
[11] F. D. C. Farrell, O. Hallatschek, D. Marenduzzo, and B. Waclaw, Phys. Rev. Lett. **111**, 168101 (2013).
[12] M. C. Marchetti, J. F. Joanny, S. Ramaswamy, T. B. Liverpool, J. Prost, M. Rao, and R. A. Simha, Rev. Mod. Phys. **85**, 1143 (2013).
[13] R. Balagam and O. A. Igoshin, PLoS Comput. Biol. **11**, 1 (2015).
[14] P. Ghosh, E. Ben-Jacob, and H. Levine, Phys. Biol. **10**, 066006 (2013).
[15] P. Ghosh, J. Mondal, E. Ben-Jacob, and H. Levine, Proc. Natl. Acad. Sci. USA **112**, E2166 (2015).
[16] C. M. Waters and B. L. Bassler, Annu. Rev. Cell Dev. Biol. **21**, 319 (2005).
[17] X. Fu, L.-H. Tang, C. Liu, J.-D. Huang, T. Hwa, and P. Lenz, Phys. Rev. Lett. **108**, 198102 (2012).
[18] S. Payne, B. Li, Y. Cao, D. Schaeffer, M. D. Ryser, and L. You, Mol. Syst. Biol. **9**, 697 (2013).
[19] B. Liebchen, D. Marenduzzo, I. Pagonabarraga, and M. E. Cates, Phys. Rev. Lett. **115**, 258301 (2015).
[20] J. S. Webb, L. S. Thompson, S. James, T. Charlton, T. Tolker-Nielsen, B. Koch, M. Givskov, and S. Kjelleberg, J. Bacteriol. **185**, 4585 (2003).
[21] Y. Tanouchi, A. Pai, N. E. Buchler, and L. You, Mol. Syst. Biol. **8**, 1744 (2012).
[22] N. Allocati, M. Masulli, C. Di Ilio, and V. De Laurenzi, Cell Death Dis. **6**, e1609 (2015).
[23] D. J. Dwyer, D. M. Camacho, M. A. Kohanski, J. M. Callura, and J. J. Collins, Mol. Cell **46**, 561 (2012).
[24] J. S. Webb, M. Givskov, and S. Kjelleberg, Curr. Opin. Microbiol. **6**, 578 (2003).
[25] P. Meier, A. Finch, and G. Evan, Nature **407**, 796 (2000).
[26] H. Engelberg-Kulka, S. Amitai, I. Kolodkin-Gal, and R. Hazan, PLoS Genet. **2**, e135 (2006).
[27] A. Erental, I. Sharon, and H. Engelberg-Kulka, PLoS Biol. **10**, e1001281 (2012).
[28] M. G. Fagerlind, J. S. Webb, N. Barraud, D. McDougald, A. Jansson, P. Nilsson, M. Harlén, S. Kjelleberg, and S. A. Rice, J. Theor. Biol. **295**, 23 (2012).
[29] J. E. González-Pastor, E. C. Hobbs, and R. Losick, Science **301**, 510 (2003).
[30] I. S. Tan, C. A. Weiss, D. L. Popham, and K. S. Ramamurthi, Dev. Cell **34**, 682 (2015).
[31] D. Claessen, D. E. Rozen, O. P. Kuipers, L. Sogaard-Andersen, and G. P. van Wezel, Nat. Rev. Micro. **12**, 115 (2014).
[32] K. Lewis, Microbiol. Mol. Biol. Rev. **64**, 503 (2000).
[33] K. W. Bayles, Nat. Rev. Micro. **12**, 63 (2014).
[34] J. W. Wireman and M. Dworkin, J. Bacteriol. **129**, 796 (1977).
[35] H. R. Meredith, J. K. Srimani, A. J. Lee, A. J. Lopatkin, and L. You, Nat. Chem. Biol. **11**, 182 (2015).
[36] C. Carmona-Fontaine and J. B. Xavier, Mol. Syst. Biol. **8**, 627 (2012).
[37] E. S. Gloag, L. Turnbull, A. Huang, P. Vallotton, H. Wang, L. M. Nolan, L. Mililli, C. Hunt, J. Lu, S. R. Osvath *et al.*, Proc. Natl. Acad. Sci. USA **110**, 11541 (2013).
[38] M. Allesen-Holm, K. B. Barken, L. Yang, M. Klausen, J. S. Webb, S. Kjelleberg, S. Molin, M. Givskov, and T. Tolker-Nielsen, Mol. Microbiol. **59**, 1114 (2006).
[39] M. Matsushita, F. Hiramatsu, N. Kobayashi, T. Ozawa, Y. Yamazaki, and T. Matsuyama, Biofilms **1**, 305 (2004).
[40] J. A. Bonachela, C. D. Nadell, J. B. Xavier, and S. A. Levin, J. Stat. Phys. **144**, 303 (2011).
[41] D. A. Kessler and H. Levine, Nature **394**, 556 (1998).
[42] S. Arouh and H. Levine, Phys. Rev. E **62**, 1444 (2000).
[43] I. Golding, Y. Kozlovsky, I. Cohen, and E. Ben-Jacob, Physica A **260**, 510 (1998).
[44] M. Godin, F. F. Delgado, S. Son, W. H. Grover, A. K. Bryan, A. Tzur, P. Jorgensen, K. Payer, A. D. Grossman, M. W. Kirschner *et al.*, Nat. Meth. **7**, 387 (2010).
[45] See Supplemental Material at http://link.aps.org/supplemental/10.1103/PhysRevE.96.052404 for the corresponding movies of the growing colonies in the absence and in the presence of cell death, as demonstrated in Fig. 2 in the main text.
[46] C. Giverso, M. Verani, and P. Ciarletta, J. R. Soc. Interface **12**, 20141290 (2015).
[47] J. Yan, A. G. Sharo, H. A. Stone, N. S. Wingreen, and B. L. Bassler, Proc. Natl. Acad. Sci. USA **113**, E5337 (2016).
[48] M.-C. Duvernoy, T. Mora, M. Ardre, V. Croquette, D. Bensimon, C. Quilliet, J.-M. Ghigo, M. Balland, C. Beloin, S. Lecuyer, *et al.*, bioRxiv. 2017, http://www.biorxiv.org/content/early/2017/01/31/104679.